

# Pattern formation in nonextensive thermodynamics: Selection criterion based on the Renyi entropy production

Olgierd Cybulski,<sup>a)</sup> Daniel Matysiak, and Volodymyr Babin

*Institute of Physical Chemistry, Polish Academy of Sciences, Kasprzaka 44/52, Warsaw 01-224, Poland*

Robert Holyst

*Institute of Physical Chemistry, Polish Academy of Sciences, Kasprzaka 44/52, Warsaw 01-224, Poland and  
Department of Mathematics and Natural Sciences, College of Science, Cardinal Stefan Wyszyński  
University, Dewajtis 5, Warsaw, 01-815, Poland*

(Received 13 December 2004; accepted 14 February 2005; published online 2 May 2005)

We analyze a system of two different types of Brownian particles confined in a cubic box with periodic boundary conditions. Particles of different types annihilate when they come into close contact. The annihilation rate is matched by the birth rate, thus the total number of each kind of particles is conserved. When in a stationary state, the system is divided by an interface into two subregions, each occupied by one type of particles. All possible stationary states correspond to the Laplacian eigenfunctions. We show that the system evolves towards those stationary distributions of particles which minimize the Renyi entropy production. In all cases, the Renyi entropy production decreases monotonically during the evolution despite the fact that the topology and geometry of the interface exhibit abrupt and violent changes. © 2005 American Institute of Physics.

[DOI: 10.1063/1.1886728]

## I. INTRODUCTION

Formation of patterns is a common phenomenon in many natural and artificial systems. For example, cellular structures in two dimensions are known in many areas of science.<sup>1</sup> We find characteristic morphological patterns in bee honeycomb, soap foam (or froth),<sup>2-4</sup> defects condensation of charge density waves,<sup>5</sup> territories of fire ants,<sup>6</sup> administrative divisions,<sup>7,8</sup> superclusters of galaxies (large scale structure of the universe),<sup>9</sup> 2D sections of polycrystalline materials, chemical patterns on surfaces, and crack structures in ceramics.<sup>10</sup> Some patterns, like those arising from crystal growth or honeycomb manufacture, are regular and predictable. Others, like crack patterns in broken glass, seem to be irregular and unpredictable. Moreover, some systems which generate patterns are intrinsically noisy and disordered. The patterns arise as a result of complex evolution of the system described usually by nonlinear (integral/differential) equations. Such patterns, when subjected to detailed quantitative morphological analysis, as in the case of 2D transition in magnetic systems,<sup>11</sup> or kinetic roughening of etched Si,<sup>12</sup> can give information about the mechanisms of their formation. It can also shed light on the selection criteria, i.e., why a certain pattern emerges and not another. In the ideal case, the selection rule is based on some variational principle. One such principle was introduced in 1957 by Jaynes.<sup>13</sup> Jaynes' principle provides a constructive criterion for setting up probability distributions on the basis of partial knowledge, and leads to a type of statistical inference which is called the maximum-entropy estimate. It is the least biased estimate possible on the given information; i.e., it is maximally non-committal with regard to missing information. If one consid-

ers statistical mechanics as a form of statistical inference rather than as a physical theory, it is found that the usual computational rules, starting with the determination of the partition function, are an immediate consequence of the maximum-entropy principle. In Jaynes' principle, we choose the appropriate entropy function (usually in the form of the Boltzmann-Gibbs-Shannon entropy), impose the constraints which follow from a partial knowledge of the system and maximize this entropy subject to the constraints. Jaynes' principle is a powerful method which allows the morphology of systems and the physical origin of the emerging pattern to be determined. For example, Jaynes' principle can be applied to such diverse phenomena as an order-disorder transition,<sup>14</sup> crack formation in broken glass,<sup>14</sup> or the formation of palladium hydrates on the surface of thin palladium film.<sup>15</sup>

There is yet another class of patterns which form away from the equilibrium. Spontaneous pattern formation can be observed in chemical reactions when the diffusion of species play a role. In the simplest case, we put two chemicals, called an activator and an inhibitor, in a dish and allow them to react and diffuse. If the inhibitor diffuses faster than the activator, the system becomes unstable. The instability manifests itself in steady concentration patterns of the reactants, corresponding to activator-rich and inhibitor-rich domains. This mechanism which leads to the pattern formation in the reaction-diffusion system, was proposed in 1952 by Turing.<sup>16</sup> The stationary regular patterns emerging in the system are called Turing patterns. The experimental evidence of two-dimensional Turing patterns was discovered in the early nineties in chloride-iodide-malonic acid (CIMA) reactions in gel media.<sup>17-21</sup> These experiments demonstrated the existence of a range of stable regular patterns. However, we are not aware of any variational principle which would explain

<sup>a)</sup>Electronic mail: olgierd@ryba.ichf.edu.pl

the formation of the patterns. Some works<sup>22</sup> indicate that the entropy production (dissipation) for various patterns in reaction-diffusion systems may be the same. They also show that the dissipation is lowered during the transition to chaotic patterns. Similarly, in other systems, like random sequential adsorption,<sup>23</sup> the entropy production rate gives the criterion for the regularity of patterns. In Rayleigh–Benard convection,<sup>24</sup> the pattern analysis is based on the spectral entropy. When we consider the motion of dislocation loops,<sup>25</sup> point defects on a line,<sup>26</sup> and chemical waves or Benard convective cells, we invariably look at various sorts of dissipation and in many cases we base the equations governing the evolution of the systems on the minimization of dissipation.<sup>14,25,26</sup> It is especially true if the system of interest is not far from the equilibrium.

Prigogine and de Groot conjectured that for open systems not far from the equilibrium the entropy production, and thus dissipation,<sup>27</sup> are minimized in the stationary states minimum entropy production (MEP). Far from the equilibrium, MEP breaks down, although part of the entropy production given by the contraction of the phase space has been shown to be minimized in some special cases.<sup>28</sup> One of the approaches to nonequilibrium statistical mechanics is related to the study of the entropy production and the escape rate of transport processes far from the equilibrium,<sup>29–32</sup> with emphasis on the Lyapunov exponents and the onset of chaos.

There are many systems in nature which do not conform to the description of classical thermodynamics, since they violate two basic thermodynamic assumptions: existence of the equilibrium state and extensivity of thermodynamic potentials. They cannot be divided into subsystems, i.e., are nonextensive, and therefore the macroscopic parameters characterizing their properties do not possess proper densities. The new approach to such systems is called nonextensive thermodynamics<sup>33,34</sup> based on the Tsallis or Renyi entropies. In recent years, there has been a search for variational principles in nonextensive thermodynamics.<sup>35</sup>

The aim of this paper is to present a simple diffusion-reaction model which can be described in terms of nonextensive thermodynamics,<sup>36</sup> with emphasis on the variational principle governing the evolution of the system. In our previous paper,<sup>36</sup> we discussed a system of Brownian particles with matching death and branching (birth) rates,<sup>37,38</sup> which minimizes the Renyi entropy production in the stationary states. Each particle performs an independent random walk inside a given region. A particle is removed after reaching the boundary of the region and, exactly at the same time, another particle (chosen at random) is duplicated. It follows that the total number of particles in the system is conserved. It was the first model studied so far which was shown to have the property of minimizing the Renyi entropy production in the stationary state. *Here we would like to extend the model to two types of particles which annihilate when they meet and show that the three-dimensional patterns emerging in such a reaction-diffusion system can be inferred from the minimization of the Renyi entropy production.*

The paper is organized as follows: in Sec. II, we define the model, the entropy, and the entropy production. In Sec. III, we discuss the stationary states of the model. In Sec. IV,

we present the detailed simulation results and show how the system reaches stationary states. Concluding remarks are given in Sec. V.

## II. THE MODEL AND THE RENYI ENTROPY

We investigate a system of Brownian particles confined in a cubic periodic box. The particles are grouped into two types, *a* and *b*. When two particles of different types meet, they instantaneously annihilate each other and disappear from the system. At the same time, when any particle of a given type is removed (due to annihilation), another particle of the same type (chosen at random) is duplicated, i.e., it gives birth to a new particle of the same type. Thus, the number of particles of each type is conserved. Diffusion, together with annihilation of particles of different types leads to the spatial segregation of particles of different types.

In the continuous limit, we can describe the process in terms of the evolution of the probability density distributions,  $p_a$  and  $p_b$ . The densities  $p_a$  and  $p_b$  satisfy the following equations:

$$\frac{\partial}{\partial t} p_a(\mathbf{r}, t) = \Delta p_a + \Lambda_a(t) p_a - k p_a p_b, \quad (1)$$

$$\frac{\partial}{\partial t} p_b(\mathbf{r}, t) = \Delta p_b + \Lambda_b(t) p_b - k p_b p_a,$$

$$\int_V p_a dV = \int_V p_b dV = 1, \quad (2)$$

where the positive constant  $k$  acts as the chemical reaction rate constant. The terms  $\Lambda_i(t) p_i(\mathbf{r}, t)$  represent “birth” of *i*-type particles at point  $\mathbf{r}$  at time  $t$ . The functions  $\Lambda_i(t)$  must be determined from the normalization condition given in Eq. (2). The mixed term  $k p_a p_b$  represents the annihilation of particles of different types. For finite values of  $k$ , the domains occupied by particles of different types partially overlap. When  $k$  increases, boundaries between the domains get sharper. In the limit of  $k \rightarrow \infty$ , we are left with a model with infinitely sharp separation of the particles of different types. The final equations are

$$\frac{\partial}{\partial t} p_a(\mathbf{r}, t) = \Delta p_a + \Lambda_a(t) p_a, \quad (3)$$

$$\frac{\partial}{\partial t} p_b(\mathbf{r}, t) = \Delta p_b + \Lambda_b(t) p_b,$$

$$\int_V p_a dV = \int_V p_b dV = 1, \quad (4)$$

$$\nabla \mathbf{r} \in V p_a p_b = 0, \quad (5)$$

where the latter condition is introduced instead of the mixed terms in Eq. (1). We have shown previously<sup>36</sup> that for a system with only one type of particle, one can describe stationary states and the evolution of the system towards the sta-

tionary states in terms of the Renyi entropy and its production. The Renyi entropy is defined as

$$S_q[p] = \frac{1}{1-q} \ln \int p^q(\mathbf{x}, t) d\mathbf{x}, \quad (6)$$

where  $p$  is the probability density distribution and  $q$  is a parameter.  $S_q$  approaches Boltzmann–Gibbs–Shannon entropy as  $q \rightarrow 1$ . In our system,  $q=2$ .<sup>36</sup> For two independent systems,  $A$  and  $B$ , the Renyi entropy is additive, i.e.,

$$S_q^R(A+B) = S_q^R(A) + S_q^R(B). \quad (7)$$

The Renyi entropy production in a system consisting of one type of particle follows from the equation for the evolution of the Renyi entropy [Eq. (6)] in time. Using Eq. (3), the time derivative  $dS/dt$  can be split into two terms,

$$\frac{dS}{dt} = \underbrace{\frac{-2 \int_V p \Delta p dV}{\int_V p^2 dV}}_{\text{entropy production, } \sigma} + 2 \underbrace{\oint \nabla p \cdot d\mathbf{S}}_{\text{outgoing flux}}, \quad (8)$$

where the first term is identified as the entropy production  $\sigma$ , and the second term as the outgoing entropy flux. Stationary distributions minimize  $\sigma$ . Moreover, in a one component system,  $\sigma$  decreases monotonically in time.

In this paper, we postulate that if the boundary between the domains occupied by different types of particles is infinitely sharp, we can, in the first approximation, treat them as independent systems. Thus, we define the total entropy as the sum of the entropies for  $a$  particles and  $b$  particles. Correspondingly, the total entropy production is given by the following sum:

$$\sigma = - \frac{2 \int_V p_a \Delta p_a dV}{\int_V p_a^2 dV} - \frac{2 \int_V p_b \Delta p_b dV}{\int_V p_b^2 dV}. \quad (9)$$

As we shall show, the stationary states chosen in the process of evolution of the system are those which minimize  $\sigma$  given by Eq. (9). Therefore, the minimization of  $\sigma$  is the variational criterion for the selection of stationary states.

### III. STATIONARY STATES

Let us consider the stationary solutions of Eq. (1). Integration of Eq. (1) over the periodic box yields

$$\Lambda_a = \Lambda_b = \Lambda. \quad (10)$$

Hence, in stationary states (as  $\partial p_a / \partial t = \partial p_b / \partial t = 0$ ) the difference  $\phi = p_a - p_b$  must be an eigenfunction of the Laplacian,

$$\Delta \phi + \Lambda \phi = 0. \quad (11)$$

From the condition  $\forall \mathbf{r} \in V p_a p_b = 0$ , we get  $(p_a + p_b)^2 = \phi^2$ . After taking the square root of both sides of the latter, one arrives at  $p_a + p_b = |\phi|$ . Thus, the stationary distributions  $p_a$

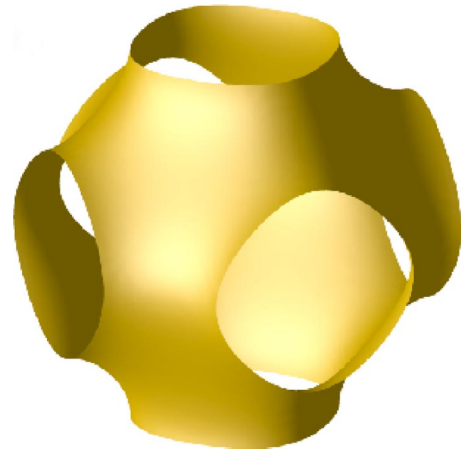


FIG. 1. Nodal approximation for triply periodic minimal surface  $P$  [see Eq. (15)].

and  $p_b$  can be expressed in terms of the Laplacian eigenfunction  $\phi$  as follows:

$$p_a = \frac{1}{2}(\phi + |\phi|), \quad p_b = \frac{1}{2}(|\phi| - \phi). \quad (12)$$

The above formulas can be written in a compact form using the Heaviside step-function  $\Theta(x)$

$$p_a = \phi \Theta(\phi), \quad p_b = -\phi \Theta(-\phi). \quad (13)$$

Thus, the surface dividing the domains of  $a$  and  $b$  is given by  $\phi=0$ .

The normalization conditions [Eq. (4)] lead to the following constraints on  $\phi$

$$\int_V d\mathbf{r} \phi = 0, \quad \int_V d\mathbf{r} |\phi| = 2. \quad (14)$$

Each solution of Eq. (11), which satisfy the above conditions, define the stationary solution of Eqs. (3)–(5). Explicit examples of the admissible eigenfunctions are given below:

$$\phi_X^s = \sin X, \quad \phi_Y^s = \sin Y, \quad \phi_Z^s = \sin Z,$$

$$\phi_X^c = \cos X, \quad \phi_Y^c = \cos Y, \quad \phi_Z^c = \cos Z,$$

where  $X=2\pi x/L$ ,  $Y=2\pi y/L$ ,  $Z=2\pi z/L$ , and  $L$  is the linear size of the periodic cubic box (constant normalization factors have been omitted for brevity). All these solutions correspond to the same eigenvalue of the Laplacian, i.e., their linear combination with arbitrary coefficients is also an admissible eigenfunction having the same eigenvalue.

For future reference, we spell three more admissible eigenfunctions explicitly,

$$\phi_P = \phi_X^s + \phi_Y^s + \phi_Z^s = \sin X + \sin Y + \sin Z, \quad (15)$$

$$\phi_D = \cos X \cos Y \cos Z + \sin X \sin Y \sin Z, \quad (16)$$

and

$$\phi_G = \sin X \cos Y + \sin Y \cos Z + \cos X \sin Z. \quad (17)$$

Functions  $\phi_P$ ,  $\phi_D$ , and  $\phi_G$  all have one interesting property, namely, the surfaces dividing  $a$  domains from  $b$  domains are

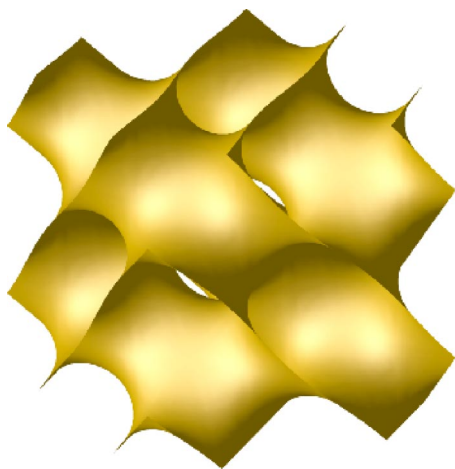


FIG. 2. Nodal approximation for triply periodic minimal surface  $D$  [see Eq. (16)].

nodal approximations to the triply periodic minimal surfaces.<sup>39–42</sup> For example,  $\phi_P=0$ , shown in Fig. 1, is the  $P$  nodal surface;  $\phi_D=0$ , shown in Fig. 2, is the  $D$  nodal surface; and  $\phi_G=0$ , shown in Fig. 3, is the  $G$  nodal surface.

#### IV. TOPOLOGICAL AND GEOMETRICAL CHARACTERISTICS OF THE DOMAIN INTERFACES

The evolution of the system can be described in terms of the evolution of the topology and geometry of the surface separating  $a$  and  $b$  domains. The topology can be quantitatively described using the Euler characteristic and/or genus. The genus  $g$  of a closed, oriented surface is the number of “handles.” The Euler characteristic is defined as  $\chi=2(1-g)$ . It is 2 for a sphere (since  $g=0$ ), 0 for a torus ( $g=1$ ), and  $-2$  for two tori joined by a handle (passage) ( $g=2$ ). The Euler characteristic for a system of disjoint surfaces is equal to the sum of the Euler characteristic of individual surfaces. If we join two surfaces by a passage, the Euler characteristic of a system will change by  $-2$ , which is easy to see. Let us take two spheres for which we have  $\chi=4$ . If we join them by a passage we will get a single closed surface with  $\chi=2$ . Therefore a passage changed  $\chi$  of the system by  $-2$ . If a droplet appears in a system, the Euler characteristic changes by  $+2$ .

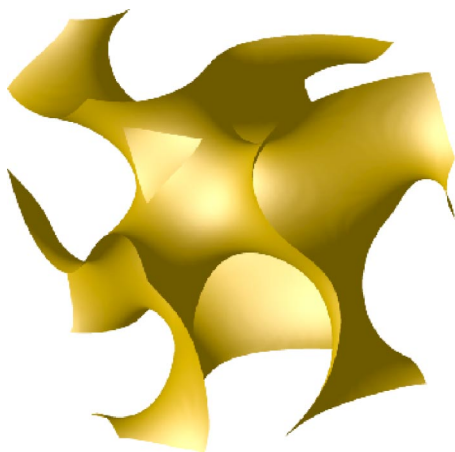


FIG. 3. Nodal approximation for triply periodic minimal surface  $G$  [see Eq. (17)].

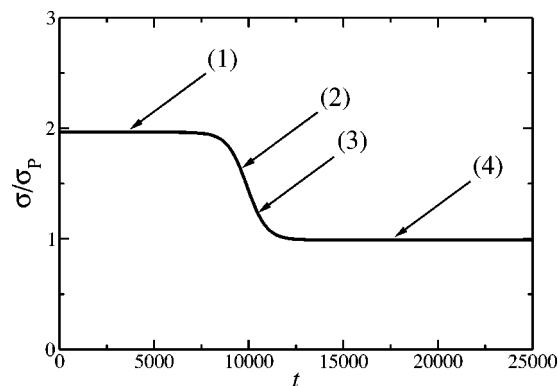


FIG. 4. Evolution of the entropy production  $\sigma$  over time. The starting configuration is  $\phi_G + \epsilon\phi_P$  ( $\epsilon=10^{-4}$ ), where  $\phi_G$  is given in Eq. (17). The snapshots of the interface separating domains of  $a$  and  $b$  in the indicated instants of time  $t$  are presented in Fig. 5. The topological and geometrical characteristics of these interfaces are gathered in Table I. The time  $t$  is measured in simulation steps. The entropy production  $\sigma$  is in units  $\sigma_P=4 \times (2\pi/L)^2$ , i.e., the entropy production for the stationary state with the symmetry and topology of nodal surface  $P$  [Eq. (15)].

Therefore we have two typical topological elements: a droplet and a passage. Finally it is possible to define the Euler characteristic for the flat interface in a periodic box. Such surface is equivalent topologically to a tori, and therefore its Euler characteristic is zero.

The surface  $\phi=p_a-p_b=0$  is reconstructed from the numerical data by the “marching tetrahedra” algorithm.<sup>11,43,44</sup> The Euler characteristics  $\chi$  is then evaluated using the Euler formula

$$\chi = \#F + \#V - \#E, \quad (18)$$

where  $\#F$ ,  $\#V$ , and  $\#E$  is the number of faces ( $\#F$ ), vertices ( $\#V$ ), and edges ( $\#E$ ), respectively, of all polygons cut by the surface. The surface area is simply the area of all polygons covering the surface. We have computed all the topological and geometrical characteristics of the system, such as the number of disjoint surfaces, their area, and Euler characteristics, using the code developed in our group.<sup>11,43,44</sup>

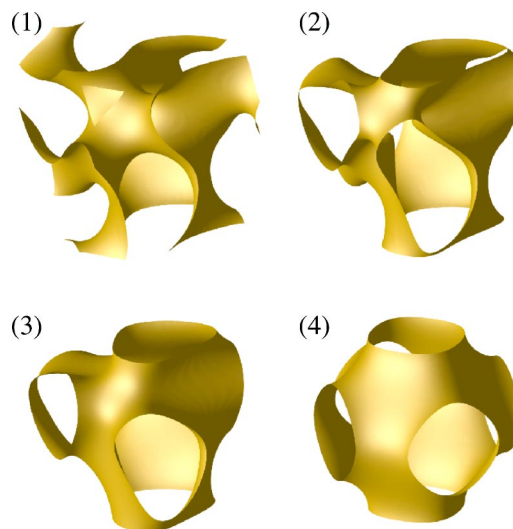


FIG. 5. The interface separating domains of  $a$  and  $b$  is shown at the time instants indicated in Fig. 4. The initial configuration is based on  $\phi_G$  [see Eq. (17)].

TABLE I. Topological and geometrical characteristics of the interface separating domains of  $a$  and  $b$ . Each row of the table corresponds to a snapshot shown in Fig. 5. In the first column, the instants of time  $t$  are given. These marks are also shown in the plot of the entropy production Fig. 4. In the subsequent columns, the number of separate surfaces  $N_s$  within the unit cell, the Euler characteristics  $\chi$ , and the surface area  $A$  are presented at the given instants of time. The surface area  $A$  is in units of  $L^2$ .

$t$	$N_s$	$A$	$\chi$
(1)	1	3.09	-8
(2)	1	2.99	-8
(3)	1	2.48	-4
(4)	1	2.35	-4

## V. NUMERICAL RESULTS

At every instant of time  $t$ , the solutions of Eq. (3) are approximated by their point values,  $p_{i,j,k}(t)$ , on the cubic lattice of size  $L \times L \times L$ . Once we have a solution at time  $t$ , we advance in time,  $t \rightarrow t + \Delta t$ , using a three-step procedure. First, we perform a diffusion step,

$$P_{a;i,j,k} \rightarrow P_{a;i,j,k} + \Delta t \nabla^2 P_{a;i,j,k}, \quad (19)$$

$$P_{b;i,j,k} \rightarrow P_{b;i,j,k} + \Delta t \nabla^2 P_{b;i,j,k},$$

where  $\nabla^2$  is the standard seven-point discrete Laplacian. Next, a reaction step is done,

$$P_{a;i,j,k} \rightarrow P_{a;i,j,k} - \min(P_{b;i,j,k}; P_{a;i,j,k}), \quad (20)$$

$$P_{b;i,j,k} \rightarrow P_{b;i,j,k} - \min(P_{b;i,j,k}; P_{a;i,j,k}),$$

where  $\min$  denotes the minimal value of its two arguments. Finally, we renormalize the probability distributions,

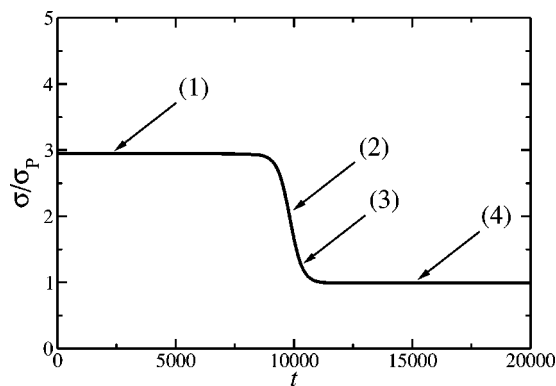


FIG. 6. Evolution of the entropy production  $\sigma$  over time. The starting configuration is  $\phi_D + \epsilon \phi_P$  ( $\epsilon = 10^{-4}$ ), where  $\phi_D$  is given in Eq. (16). The snapshots of the interface separating domains of  $a$  and  $b$  in the indicated instants of time  $t$  are presented in Fig. 7. The topological and geometrical characteristics of these interfaces are gathered in Table II. The time  $t$  is measured in simulation steps. The entropy production  $\sigma$  is in units  $\sigma_P = 4 \times (2\pi/L)^2$ , i.e., the entropy production for the stationary state with the symmetry and topology of surface  $P$  [Eq. (15)].

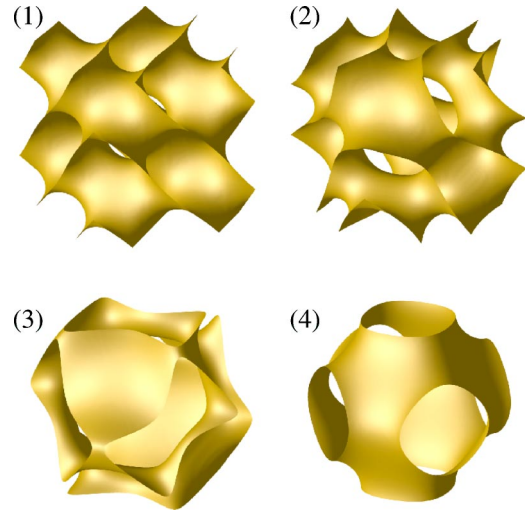


FIG. 7. The interface separating domains of  $a$  and  $b$  is shown at the time instants indicated in Fig. 6. The initial configuration is based on  $\phi_D$  [see Eq. (16)].

$$P_{a;i,j,k} \rightarrow \frac{P_{a;i,j,k}}{\sum_{i,j,k} P_{a;i,j,k}}, \quad (21)$$

$$P_{b;i,j,k} \rightarrow \frac{P_{b;i,j,k}}{\sum_{i,j,k} P_{b;i,j,k}},$$

where the summation runs over all lattice points. The last step guarantees that the normalization of the probabilities is preserved during the evolution.

The validity of the numerical procedures has been checked by preparing initial distributions  $p_a$  and  $p_b$  in such a way so as to assure that  $p_a - p_b$  is an admissible eigenfunction of the Laplacian. Simulations confirmed that such configurations are stationary, i.e., they do not change in time. The values of the entropy production, evaluated numerically, have been found to agree with their analytical counterparts (<2% error for a cubic lattice of size  $64 \times 64 \times 64$ ).

We have computed the evolution of the system starting from different initial configurations. In all cases, the final distributions, reached after a sufficiently long time, corresponded to a linear combination of  $\phi_X^{c,s}$ ,  $\phi_Y^{c,s}$ , and  $\phi_Z^{c,s}$ , provided that the initial configuration was not based on one of the Laplacian eigenfunctions. As it was expected, long-living structures, encountered during evolution, correspond to stationary solutions described in Sec. III. The transitions between the configurations proceed exponentially fast. Only probability distributions corresponding to a linear combina-

TABLE II. Characteristics related to Figs 6 and 7. Notation and units as in Table I.

$t$	$N_s$	$A$	$\chi$
(1)	1	3.84	-16
(2)	1	3.62	-16
(3)	1	2.78	-4
(4)	1	2.35	-4

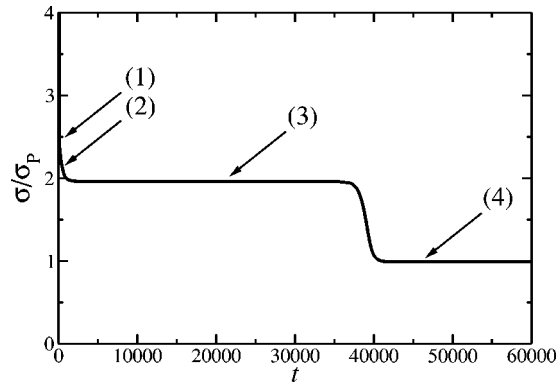


FIG. 8. Evolution of the entropy production  $\sigma$  over time. The starting configuration has the symmetry and topology of surface I-WP [Eq. (22)]. The snapshots of the interface separating  $a$ - and  $b$ -rich domains in the indicated instants of time  $t$  are presented in Fig. 9. The topological and geometrical characteristics of these interfaces are gathered in Table III. The time  $t$  is measured in simulation steps. The entropy production  $\sigma$  is in units  $\sigma_P=4 \times (2\pi/L)^2$ , i.e., the entropy production for the stationary state with the symmetry and topology of surface  $P$  [Eq. (15)].

tion of  $\phi_X^{c,s}$ ,  $\phi_Y^{c,s}$ , and  $\phi_Z^{c,s}$  were found to be stable with respect to small perturbations. What is more important is that the Renyi entropy production, defined in Eq. (9), was observed to monotonically decrease in time  $t$ . Examples of the numerical simulations for  $L=64$  are discussed below.

#### A. Initial state with topology of the $G$ surface

We start from  $p_a$  and  $p_b$  initialized using Eq. (13) with  $\phi = \phi_G$ , defined in Eq. (17). We do not observe any changes of this state in the course of simulation, because this state is the stationary solution of Eq. (3). However, if we set the initial configuration in the form  $\phi_G + \epsilon\phi_P$  (we used  $\epsilon \sim 10^{-4}$ ), then the system drops into the state corresponding to  $\phi_P$ . This indicates that  $\phi_G$  is in fact unstable. It also corroborates the proposed conjecture because the entropy production in the stationary state built upon  $\phi_G$  is indeed greater than in the case of  $\phi_P$ . The initial perturbation grows exponentially

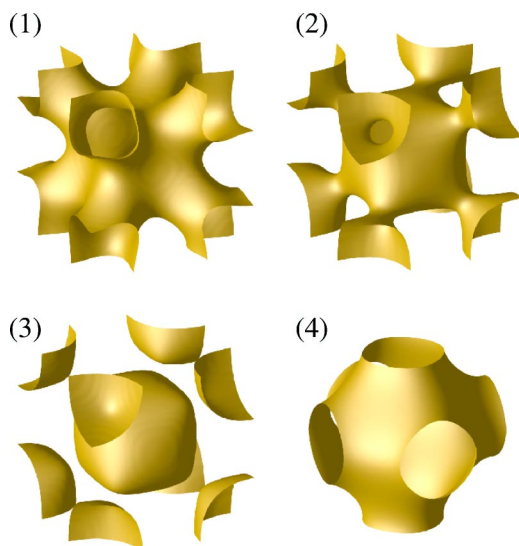


FIG. 9. The interface separating domains of  $a$  and  $b$  is shown at the time instants indicated in Fig. 8. The initial configuration is based on  $\phi_{I-WP}$  [see Eq. (22)].

TABLE III. Characteristics related to Figs. 8 and 9. Notation and units as in Table I.

$t$	$N_s$	$A$	$\chi$
(1)	1	3.55	-12
(2)	1	3.36	-12
(3)	2	0.606	2
		2.16	2
(4)	1	2.35	-4

in time with exponent proportional to the difference between the corresponding entropy productions  $\sigma_G$  and  $\sigma_P$ . The time dependence of the entropy production is shown in Fig. 4. For  $L=64$ , the value of the first plateau, where the system is in the configuration corresponding to  $\phi_G$ , is  $\sigma \approx 7.86 \times (2\pi/L)^2$ , which is close to the exact value  $8 \times (2\pi/L)^2$ . (From this point on, the entropy production is given in units of  $\sigma_P=4 \times (2\pi/L)^2$ .) The distribution then quickly evolves in such a way as to minimize the entropy production and drops into the configuration corresponding to  $\phi_P$  accordingly. Some selected snapshots from the evolution are presented in Fig. 5. The snapshots were taken at points indicated in the plot of the entropy production (Fig. 4). The topological and geometrical characteristics of the interface, at the same instants of time, are gathered in Table I.

#### B. Initial state with topology of the $D$ surface

Like in the case of  $\phi_G$ , the state based on  $\phi_D + \epsilon\phi_P$  is unstable. As long as  $\epsilon \ll 1$ , the configuration remains visibly

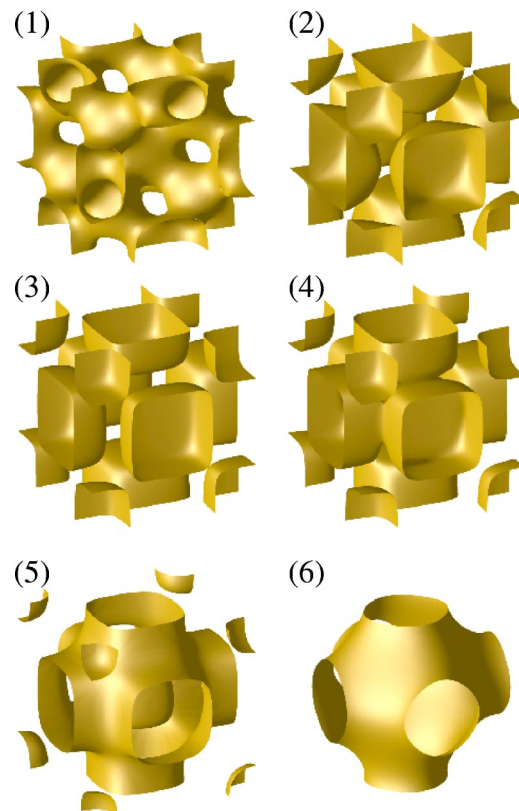


FIG. 10. The interface separating domains of  $a$  and  $b$  is shown at the time instants indicated in Fig. 11. The initial configuration is based on  $\phi_{F-RD}$  [see Eq. (23)].

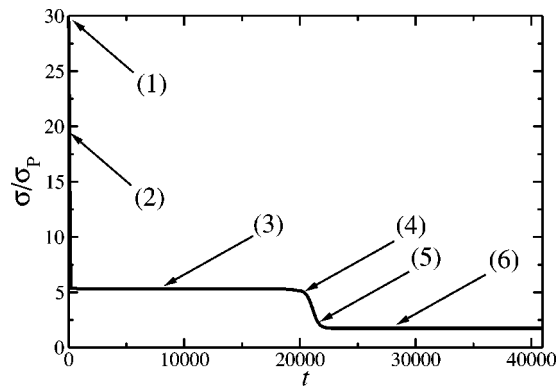


FIG. 11. Evolution of the entropy production  $\sigma$  over time. The starting configuration has the symmetry and topology of surface F-RD [Eq. (23)]. The snapshots of the interface separating  $a$ - and  $b$ -rich domains in the indicated instants of time  $t$  are presented in Fig. 10. The topological and geometrical characteristics of these interfaces are gathered in Table IV. The time  $t$  is measured in simulation steps. The entropy production  $\sigma$  is in units  $\sigma_p = 4 \times (2\pi/L)^2$ , i.e., the entropy production for the stationary state with the symmetry and topology of surface  $P$  [Eq. (15)].

unchanged, with  $\sigma \approx 2.95 \times \sigma_p$  (the exact value is  $3 \times \sigma_p$ ). However, given enough time, the system switches to the configuration corresponding to  $\phi_p$ . The plot of the evolution of the entropy production is presented in Fig. 6, whereas Fig. 7 contains selected snapshots of the system at the labeled points in Fig. 6. Rows in Table II also correspond to these points.

### C. Initial states with topology of the I-WP and F-RD surfaces

Let us examine the initial configurations for which the interfaces are nodal approximations of triply periodic minimal surfaces I-WP and F-RD. In contrast to the two previous examples, the initial configurations  $\phi_{I-WP}$  and  $\phi_{F-RD}$  are not the eigenfunctions of the Laplacian

$$\begin{aligned} \phi_{I-WP} = & 2 \cos(X)\cos(Y) + 2 \cos(Y)\cos(Z) \\ & + 2 \cos(Z)\cos(X) - \cos(2X) - \cos(2Y) - \cos(2Z) \end{aligned} \quad (22)$$

$$\begin{aligned} \phi_{F-RD} = & 12 \cos(X)\cos(Y)\cos(Z) - 2 \cos(2X)\cos(2Y) \\ & - 3 \cos(2Y)\cos(2Z) - 3 \cos(2Z)\cos(2X). \end{aligned} \quad (23)$$

The plot of the evolution of the entropy production in the case of I-WP is shown in Fig. 8. The snapshots of the interface which separates domains  $a$  and  $b$ , taken at the indicated instants of time, can be seen in Fig. 9. The topological and geometrical characteristics of the interface at these instants are given in Table III. It can be seen that the initial configuration decays rapidly, contrary to the previous two cases. It drops directly to some long-living state, shown in Fig. 9(3), characterized by  $\sigma = 2.95 \times \sigma_p$ . A similar value of the entropy production has been observed in the case of  $\phi_D$ . The system continues to evolve in much the same way as the system described in Sec. V B, eventually finishing in configuration  $\phi_p$ .

Starting from  $\phi_{F-RD}$ , we observe similar behavior; the system also drops directly from its initial configuration into a

TABLE IV. Characteristics related to Figs. 10 and 11. Notation and units as in Table I.

$t$	$N_s$	$A$	$\chi$
(1)	1	4.86	-40
(2)	1	4.82	-40
(3)	1	5.89	-40
(4)	3	0.0335	2
		2.39	-4
		0.0335	2
(5)	3	0.143	2
		2.41	-4
		0.143	2
(6)	1	2.35	-4

long-living state which eventually decays into  $\phi_p$ . Interestingly, this system, as the previous one, remains metastable with the same value of entropy production as the configuration  $\phi_D$ . The fact that these different initial configurations lead to the same entropy production in their transient metastable states is due to the degeneracy of the corresponding Laplacian eigenfunctions. Snapshots of the evolution initiated from  $\phi_{F-RD}$  are shown in Fig. 10 at points indicated in Fig. 11. Table IV presents the topological and geometrical characteristics.

The above examples, as well as numerous simulations which we have performed, confirm that the Renyi entropy production decreases monotonically in time, irrespective of the initial configuration.

## VI. CONCLUSIONS

The irreversible entropy production is one of the key quantities in nonequilibrium thermodynamics.<sup>45</sup> For systems far from the equilibrium there are no variational principles which could be used to predict the system state. The thermodynamic equilibrium is well described by thermodynamics and statistical mechanics, yet similar description for non-equilibrium states does not exist despite more than 100 years of research. It might be that the attempts to extend statistical mechanics and thermodynamics to systems far from the equilibrium relied heavily on the existence of the equilibrium state. In particular the equilibrium state was always invoked as the reference state. It might be that the description of states far from the equilibrium requires a different approach, such as proposed by Tsallis.<sup>34</sup>

In this paper we have described a simple system which, by definition, does not have an equilibrium state. Nonetheless we have shown that such system can be described and analyzed in terms of the nonextensive Renyi entropy and its production. We have been able to show that, among all possible stationary states, the system chooses those which minimize the Renyi entropy production. The reference state for any state realized in the system is the stationary state. We hope that our work will stimulate a further search for variational approaches to systems far from the equilibrium.

## ACKNOWLEDGMENTS

This work was supported by the KBN Grant No. 2P03B00923 (2002–2005).

- <sup>1</sup>D. Weaire and N. Rivier, *Contemp. Phys.* **25**, 59 (1984).
- <sup>2</sup>J. Stavans and J. A. Glazier, *Phys. Rev. Lett.* **62**, 1318 (1989).
- <sup>3</sup>A. Hamsy, R. Paredes, O. Sonnevile-Aubrun, B. Cabane, and R. Botet, *Phys. Rev. Lett.* **82**, 3368 (1999).
- <sup>4</sup>A. A. Kader and J. C. Earnshaw, *Phys. Rev. Lett.* **82**, 2610 (1999).
- <sup>5</sup>H. H. Weitering, J. M. Carpinelli, A. P. Melechko, J. D. Zhang, M. Bartkowiak, and E. W. Plummer, *Science* **285**, 2107 (1999).
- <sup>6</sup>E. S. Adams, *Ecology* **79**, 1125 (1998).
- <sup>7</sup>G. L. Caër and R. Delannay, *J. Phys. I* **3**, 1777 (1993).
- <sup>8</sup>L. Glass and W. R. Tobler, *Nature (London)* **233**, 67 (1971).
- <sup>9</sup>P. Coles, *Nature (London)* **346**, 446 (1990).
- <sup>10</sup>W. Korneta, S. K. Mendiratta, and J. Menteiro, *Phys. Rev. E* **57**, 3142 (1998).
- <sup>11</sup>M. Fialkowski and R. Holyst, *Phys. Rev. E* **66**, 046121 (2002).
- <sup>12</sup>M. E. R. Dotto and M. U. Kleinke, *Physica A* **295**, 149 (2001).
- <sup>13</sup>E. T. Jaynes, *Phys. Rev.* **106**, 620 (1957); **108**, 171 (1957).
- <sup>14</sup>M. Fialkowski and R. Holyst, *Phys. Rev. E* **65**, 057105 (2002).
- <sup>15</sup>M. Fialkowski, R. Nowakowski, and R. Holyst, *J. Phys. Chem. B* **108**, 7373 (2004).
- <sup>16</sup>A. M. Turing, *Philos. Trans. R. Soc. London, Ser. B* **273**, 37 (1952).
- <sup>17</sup>V. Castets, E. Dulos, J. Boissonade, and P. De Kepper, *Phys. Rev. Lett.* **64**, 2953 (1990).
- <sup>18</sup>P. De Kepper, V. Castets, E. Dulos, and J. Boissonade, *Physica D* **49**, 161 (1991).
- <sup>19</sup>Q. Ouyang and H. L. Swinney, *Nature (London)* **352**, 610 (1991).
- <sup>20</sup>Q. Ouyang and H. L. Swinney, *Chaos* **1**, 411 (1991).
- <sup>21</sup>Q. Ouyang, Z. Noszticzius, and H. L. Swinney, *J. Phys. Chem.* **96**, 6773 (1992).
- <sup>22</sup>M. Alghoul and B. C. Eu, *Physica D* **97**, 531 (1996).
- <sup>23</sup>N. V. Brilliantov, Y. A. Andrienko, P. L. Krapivsky, and J. Kurths, *Phys. Rev. Lett.* **76**, 4058 (1996).
- <sup>24</sup>R. V. Cakmur, D. A. Egolf, B. B. Plappand, and E. Bodenschatz, *Phys. Rev. Lett.* **79**, 1853 (1997).
- <sup>25</sup>P. Oswald, P. Pieranski, F. Picano, and R. Holyst, *Phys. Rev. Lett.* **88**, 015503–1 (2002).
- <sup>26</sup>R. Holyst and P. Oswald, *Phys. Rev. E* **65**, 041711 (2002).
- <sup>27</sup>S. R. de Groot and P. Mazur, *Non-Equilibrium Thermodynamics* (Dover, New York, 1984).
- <sup>28</sup>D. J. Evans and A. Baranyai, *Phys. Rev. Lett.* **67**, 2597 (1991).
- <sup>29</sup>W. Breymann, T. Tel, and J. Vollmer, *Phys. Rev. Lett.* **77**, 2945 (1996).
- <sup>30</sup>J. Volmer, T. Tel, and W. Breymann, *Phys. Rev. Lett.* **79**, 2759 (1997).
- <sup>31</sup>P. Gaspard and G. Nocolis, *Phys. Rev. Lett.* **65**, 1693 (1990).
- <sup>32</sup>J. Vollmer, L. Matyas, and T. Tel, *J. Stat. Phys.* **109**, 875 (2002).
- <sup>33</sup>J. A. S. Lima, R. Silva, and A. R. Plastino, *Phys. Rev. Lett.* **86**, 2938 (2001).
- <sup>34</sup>C. Tsallis, *J. Stat. Phys.* **52**, 479 (1988).
- <sup>35</sup>A. G. Bashkurov, *Phys. Rev. Lett.* **93**, 130601 (2004).
- <sup>36</sup>O. Cybulski, V. Babin, and R. Holyst, *Phys. Rev. E* **69**, 016110 (2004).
- <sup>37</sup>K. Burdzy, R. Holyst, D. Ingerman, and P. March, *J. Phys. A* **29**, 2633 (1996).
- <sup>38</sup>K. Burdzy, R. Holyst, and P. March, *Commun. Math. Phys.* **214**, 679 (2001).
- <sup>39</sup>H. G. von Schnering and R. Nesper, *Angew. Chem.* **26**, 1059 (1987); *Z. Phys. B: Condens. Matter* **83**, 407 (1991).
- <sup>40</sup>A. L. Mackay (1993), *Proc. R. Soc. London, Ser. A* **442**, 47 (1993).
- <sup>41</sup>J. Klinowski, A. L. Mackay, and H. Terrones, *Philos. Trans. R. Soc. London, Ser. A* **354**, 1975 (1996).
- <sup>42</sup>E. A. Lord and A. L. Mackay, *Curr. Sci.* **85**, 346 (2003).
- <sup>43</sup>A. Aksimentiev, M. Fialkowski, and R. Holyst, *Adv. Chem. Phys.* **121**, 141 (2002).
- <sup>44</sup><http://www.ichf.edu.pl/mfialkowski/morph.html>
- <sup>45</sup>L. Rondoni and E. G. D. Cohen, *Physica D* **168**, 341 (2002).